UM-P-93/84

Density Dependent Effective Interactions.

P. J. Dortmans and K. Amos

School of Physics, University of Melbourne, Parkville, 3052 Victoria Australia

Abstract

An effective nucleon–nucleon interaction is defined by an optimal fit to select on– and half–off–of–the–energy shell t– and g–matrices determined by solutions of the Lippmann–Schwinger and Brueckner–Bethe–Goldstone equations with the Paris nucleon–nucleon interaction as input. As such, it is seen to better reproduce the interaction on which it is based than other commonly used density dependent effective interactions. This new (medium modified) effective interaction when folded with appropriate density matrices, has been used to define proton–^{12}C and proton–^{16}O optical potentials. With them elastic scattering data are well fit and the medium effects identifiable.

I. INTRODUCTION

Over the years many groups have studied the elastic scattering of nucleons from nuclei by using model two nucleon (NN) g–matrices to describe the interactions between the projectile and constituent nucleons of the target [1–10]. Broadly, those studies may be classified into two groups, namely the set that used momentum space [2–4]and the set that used coordinate space [5–10] representations. These two approaches each have their own differing advantages. By using momentum space, non localities due to proper consideration of antisymmetrisation within the NN g–matrices can be considered as their inclusion is straight forward. But as yet, no calculation of that type has been properly considered all of the known nuclear medium modifications that define the NN g–matrices to be distinctively different to the free particle NN t–matrices. On the other hand, coordinate space studies have allowed for such medium modifications in NN g–matrices and, we consider aspects of this approach herein.

All coordinate representation studies of the nucleon–nucleus (N–A) optical potentials begin by defining effective interactions to the actual NN g–matrices. Those effective interactions can have diverse operator character (central, tensor, two body spin–orbit etc.) but always have relatively simple local functional forms (i.e. sum of Yukawas or Gaussians). Furthermore the exchange amplitudes arising from antisymmetrisation in coordinate space approach are approximated usually to give in finality, a local equivalent N–A optical model potential. Nevertheless, with such an approach, elastic scattering data can be described quite well [7,11,12] and there are noticeable effects caused by the medium modifications set into the effective NN interactions.

In the last decade, three effective interactions have received some attention. They are those which are commonly known as the LF (Love-Franey) [6], the Hamburg [7] and the $M3Y$ [13] with the last, when modified to add density effects, specified as the $DDM3Y$ [14,15]. The LF effective interaction was based upon the on–shell free NN t–matrices (the NN scattering amplitudes) as defined by the Arndt phase shifts. No constraints were applied

to the off energy shell properties of the t–matrices or to allow for medium modifications of those t–matrices specifically. But that effective interaction was designed with impulse approximation conditions in mind. In contrast, the Hamburg interaction was based upon g–matrix elements associated with the Paris interaction and evaluated allowing for Pauli blocking and, very approximately, the average background mean field in which the nucleons move. Those t–matrices were cast as functions of relative coordinates (for each NN channel) whose Fourier transformations were then mapped against those of an (coordinate space) effective interaction. This interaction was structured as central, tensor and spin–orbit in character, each with (fixed range) Yukawa form factors. The ranges were chosen *a priori* and the strengths optimised to minimise the integrated squared difference between g–matrices and those effective interaction values in the range of momentum transfer to 5 fm^{-1}. The proton–nucleus optical model potentials were then deduced by folding and reasonable results were obtained for scattering from ^{12}C. The $M3Y$ effective interaction [13] and its density dependent upgrades [14,15] are of more recent use in analyses of heavy ion interactions. That interaction and its modifications are again taken as the linear combination of Yukawa factors with long and short ranges chosen to give the $OPEP$ tail and to simulate heavy meson exchanges. The purely real strengths were selected to give g–matrix elements similar to those of the Reid soft core potential which are appropriate to describe the ^{16}O ground state. The density dependence of the $M3Y$ is then specified as a scale function, $f(\rho)$, upon the original effective interaction. Details of that function $f(\rho)$ were chosen to reproduce the density dependences of a previously calculated microscopic (N–A) optical model [16]. But this effective interaction is purely real and optical potentials derived with it then must be supplemented by a phenomenological imaginary part.

Thus by their construction and/or by the choice of constraints to fit parameter values, all these effective interactions do not truly provide a detailed representation of the NN dynamics underlying a "parameter free" theoretical model of nucleon–nucleus scattering. Recently [17] a new scheme was proposed to define effective interactions of appropriate form and which allows one to optimise fits to a range of on– and half–off–shell g–matrices. We

have used that scheme to determine effective interactions to both t– and g–matrices obtained from the Paris interaction [18] for a number of two nucleon angular momentum channels and for a range of densities up to nuclear saturation ($k_f = 1.4 fm^{-1}$). The results have been used via a local density approximation, to define the p–^{12}C and p–^{16}O optical potentials at 200 MeV. The program DWBA91 of Raynal [19] has been used to give those optical potentials and to evaluate the differential cross–sections and analysing powers.

Following a brief summary detailing the method by which the g–matrices were evaluated, and how the effective interaction parameter values were obtained , the zero density (free particle) t–matrices given by exact solution of the Lippmann–Schwinger equation starting with the Paris interaction are compared with those of our effective interaction and also with those of the Hamburg one since that is the most appropriate of the three others discussed for 200 MeV protons. Finally, we compare the optical potentials, cross–sections and analyzing powers we obtain by folding of our effective interaction with data and those results found when all medium modifications are ignored.

II. FROM T– AND G–MATRICES TO EFFECTIVE INTERACTIONS

Non–relativistic many body theories of the nucleon–nucleus optical potentials are framed around the NN t–matrices which, in momentum space and for channels α $\{= JST\}$, are solutions of the Lippmann–Schwinger equation

$$t^{(\alpha)}_{LL'}(p',p;k) = V^{(\alpha)}_{LL'}(p',p) + \frac{2}{\pi}\sum_l \int_0^\infty V^{(\alpha)}_{Ll}(p',q)\frac{q^2 dq}{q^2-k^2+i\epsilon} t^{(\alpha)}_{lL'}(q,p;k), \quad (1)$$

with k being the on–shell momentum

As in the Hamburg [7] studies, we use the Paris interaction for the $V^{(\alpha)}_{LL'}(p',p)$ and solve Eq. (1) by matrix inversion [20]. Half off of the energy shell for 200 MeV incident energy and a select set of NN channels, the t–matrices so found are given in figures 1–4 by the solid curves.

If the struck nucleon is embedded in a nuclear medium then it is more appropriate to use medium modified NN g–matrices in optical model calculations and the g–matrices used here are solutions of the Brueckner–Bethe–Goldstone (BBG) equation,

$$G^{(\alpha)}_{LL'}(p',p;k,k_f) = V^{(\alpha)}_{LL'}(p',p) + \frac{2}{\pi}\sum_l \int_0^\infty V^{(\alpha)}_{Ll}(p',q)\frac{\bar{Q}(q,K;k_f)q^2dq}{\bar{E}(q,K;k_f)-\bar{E}(k,K;k_f)+i\epsilon}G^{(\alpha)}_{lL'}(q,p;k,k_f), \quad (2)$$

wherein $\bar{Q}(q,K;k_f)$ is the (angle averaged) Pauli operator as defined previously [20] and with K being the average centre of mass momentum for a laboratory incident momentum p_o, and fermi momentum k_f *viz.*

$$\begin{aligned} K(k;k_f,p_o) &= (k^2+p_o^2)^{\frac{1}{2}} \text{ if } 0 \le 2k \le k_f - p_o \\ &= \left\{(k^2+p_o^2) - \frac{1}{4}\left[(2k+p_o)^2 - k_f^2\right]\right\}^{\frac{1}{2}} \\ &\quad \text{if } k_f - p_o \le 2k \le k_f + p_o. \end{aligned} \quad (3)$$

The energies in the propagators of the BBG equations include auxiliary potentials, U, and are defined by

$$\bar{E}(q,K;k_f) = (\frac{\hbar^2}{m})(q^2+K^2) + U(|\mathbf{q}+\mathbf{K}|) + U(|\mathbf{q}-\mathbf{K}|). \quad (4)$$

Details of the calculations have been given previously [21] and the result is tables of complex numbers for each incident energy, fermi momentum value and set of relative momenta for each NN channel. A simplification has been used in generation of those tables, namely that the struck nucleon momentum has been fixed at the averaged value of 0.85773 k_f for each density.

Those tables are the input data base for the effective interaction parametrisation scheme [17] we use herein. Specifically we have selected the half–off–shell t– and g–matrix elements in the procedure to find an optimum effective interaction which, in coordinate space, has the form

$$\begin{aligned} g^{(i)ST}_{eff}(r,E;k_f) &= \sum_{j=1}^{n_i} S^{(i)}_j(E)\frac{e^{-(r/\lambda^{(i)}_j)}}{r} \\ &= \sum_{j=1}^{n_i} S^{(i)}_j(E;k_f)\frac{e^{-\mu^{(i)}_j r}}{r}, \end{aligned} \quad (5)$$

for each operator of the set (i) = {central, tensor and two–body spin–orbit} where $S_j^{(i)}(E)$ are the complex, energy dependent strengths, and $\lambda_j^{(i)} = 1/\mu_j^{(i)}$ are the ranges of the (n_i) Yukawa functions. This effective interaction then is expressed in the form of projection operators onto each NN channel and when double Bessel transformed are defined as $g_{eff}^{(\alpha)}(p', p; E, k_f)$. The selected sets ($n_i \leq 4$ suffice) of ranges and strengths are then defined by finding an optimal fit to the actual (half–off–shell) g–matrices in the set of NN channels considered important. To facilitate this task we assume that the ranges of the Yukawa form factors are independent of both energy and density (fermi momentum) and so the first step is to optimise them prior to defining the best set of complex strengths for a given energy, density and for each spin–isospin channel. Across an energy spectrum of up to 450 MeV, the (inverse) ranges (μ_i) we have selected are (0.71, 1.758, 2.949 and 4.0 fm^{-1}) for the central components and (1.25, 2.184, 3.141 and 4.0 fm^{-1}) for both the tensor and two–body spin–orbit attributes. However, the system of equations in this mapping scheme is grossly overdetermined and there are other "optimal" sets of parameters that give equally good fits [22]. But the key factor which we stress herein is that the resultant effective interaction must remain a good representation of the NN t– and g–matrices central in a microscopic theory of the optical potential. Neither the LF or $M3Y$ (modified) are of that form. They are predicated, in the end, upon fitting many nucleon data. The original Hamburg interaction [7] did seek to remain "faithful" although in a somewhat limited fashion being determined with respect to on–shell properties only.

III. COMPARISON OF EFFECTIVE INTERACTIONS

Herein we compare the zero fermi momentum (free) Paris NN effective interactions (Hamburg and ours) with the solutions, half off of the energy shell and at 200 MeV, of the Lippmann–Schwinger equations in select NN channels. We compare only zero fermi momenta results as the two effective interactions should have that case most in common.

The half–off–of–the–energy–shell t–matrices determined by solutions of the LS equations

for diverse two nucleon channels (JST) and with the Paris interaction [18] are shown in figures 1 to 4, and in all cases, by a continuous line. The on-shell momenta of 1.55 fm^{-1} (200 MeV in the lab. frame) is displayed therein by the large dot. The dashed and dotted curves in those figures display the half-off-shell representations of those t-matrices given by our effective interactions and those of the Hamburg group [7] respectively. The real and imaginary components are displayed separately in each diagram.

The dominant spin singlet channels at 200 MeV are the $^1P_1$ (S=0,T=0) and $^1S_0$ (S=0,T=1) and the Paris t-matrices and the effective interaction representations of them are displayed in figure 1. Clearly our effective interactions reproduce the actual ones very well. The Hamburg results are quite reasonable as well over the range of off-shell momenta shown.

The important S=1,T=1 channels are the $^3P_{0,1}$ ones and the t-matrices for them are compared in figure 2. Our effective interaction reproduces the Paris t-matrices very well while the Hamburg ones are rather different. That is also the case for the deuteron channels (the S=0,T=0 t-matrices) as shown in figure 3. The Hamburg interaction does not give the appropriate half-off-shell $^3S_1$ t-matrix elements and neither effective interaction well reproduce those of the $^3D_1$ channel. Overall, however, we contend that our interaction is the better candidate in these coupled channels. But that is not necessarily the case in all channels and the $^3D_2$ is a case in question. The $^3D_2$ half-off-shell t-matrices are compared in figure 4. Therein it is evident that while both effective interactions are poor descriptions of the actual Paris t-matrix, ours is the worse.

IV. DENSITY EFFECTS ON ELASTIC SCATTERING

We have used our effective interaction to calculate the local, optical model potentials for the scattering of 200MeV protons from ^{12}C and ^{16}O. The code DWBA91 [19] has been used for that purpose with a Fermi distribution

$$\rho_f(r) = \frac{\rho_o}{1 + e^{(r-c)/a}} \tag{6}$$

defining the local fermi momenta that specifies the NN g–matrices in a local density approximation. Parameter values of k_f=1.29 fm^{-1} (to define ρ_o), c=1.025$A^{\frac{1}{3}}$ fm and a=0.55 fm as defined previously [23] were used and the ^{12}C ground state was set by a complete 0s–shell and 8 (4 proton, 4 neutron) 0p–shell nucleons each described by harmonic oscillator functions for an oscillator length of 1.64 fm. In the case of ^{16}O, the Fermi distribution was fit with k_f=1.31 fm^{-1}, c=1.030$A^{\frac{1}{3}}$ fm and a=0.55 fm, while a harmonic oscillator length of 1.76 fm was used.

The DWBA91 code uses a local approximation for the exchange amplitudes and the resultant local potentials are displayed in figure 5 for ^{12}C and in figure 6 for ^{16}O. The central and spin–orbit potentials we obtained are shown in the top and bottom segments respectively with the real and imaginary parts indicated. The solid curves are the results found when our density dependent effective interaction is used. The dashed curves are the results given when the effective interaction to the free NN (Paris) t–matrices is used i.e. all medium modification effects are turned off. The medium modifications to the central potentials show a significant reduction in the absorption while there is an increase in the real (refractive) part. On the scales shown, these variations are not evidently severe but they are of absolute values far an excess of the changes to the spin–orbit potentials caused by the same medium modifications. Even so the real and imaginary parts of the spin–orbit potentials are quite markedly affected by the medium effects. Notably, the more realistic interaction is less absorptive and located more within the nuclear matter distribution when compared with the potential deduced by using the effective interaction to the free NN t–matrices.

The results of our calculations of the elastic scattering of 200 MeV protons from ^{12}C and ^{16}O are shown in figures 7 and 8 respectively. Therein, the differential cross–section and analyzing power data for ^{12}C [11] and ^{16}O [12] are compared with the results found using the effective interaction to the NN g–matrices that are given by the continuous curve. The results found by using our effective interactions to the free (Paris) NN t–matrices are displayed by the dashed curves. Use of the density dependent effective interaction gives a

demonstrably better fit to the data than does use of the free NN t–matrix model. In the cross–section fit, the χ^2 per degree of freedom is a factor of 2 to 3 improved while that of the analyzing power is reduced almost by an order of magnitude.

V. CONCLUSION

Many studies have stressed the need to have effective NN interactions for use in microscopic model evaluations of (local) nuclear optical potentials that are based upon realistic free two nucleon scattering interactions, that properly reflect the off–shell character of the t matrices given by those realistic NN interactions and that account for medium modifications to those t–matrices. But few, however, have taken all of the defined constraints into account. Of those that do, most if not all have not considered both Pauli blocking and average field facets of the medium corrections, but, more problematically, have used effective interactions that do not sufficiently well reproduce the off–shell g–matrices to which they were fit. The density dependent Hamburg interaction while being very useful in past analyses of N–A scattering data, is such an example. It does not give a satisfactory representation of the zero density (free NN), Paris t–matrices upon which it was based. But an effective interaction scheme developed recently can be used to give an equally utilitarian form. Our results when it is used for the zero density limit are better representations of the half–off–shell Paris t–matrices (at 200 MeV) for most low J NN channels. The mapping is so overdetermined however that not all channel results are good – or even better representations – than the Hamburg ones.

Neglecting medium corrections gave optical model potentials that led to a reasonable description of the differential scattering cross–sections in two test cases; 200 MeV protons from ^{12}C and ^{16}O. But the analyzing power prediction is quite poor. On the other hand, by using an effective interaction that gave comparable fits to the half–off–shell g–matrix elements computed with both Pauli blocking and average field effects in the relevant BBG equations, the attendant optical potentials for 200 MeV protons on both nuclei led to better

fits to the differential cross-section data and a very much better ones to the measured analysing power.

Thus we reconfirm the conclusions of others that there is a marked effect of density dependence in effective interactions upon the specifications of nucleon optical potentials, but we establish that with a more realistic representation of the relevant NN g–matrices.

VI. ACKNOWLEDGEMENTS

We are grateful to Dr. J. Raynal and Prof. H. V. von Geramb for allowing us the use of their codes, and to Drs. P. Schwandt and J. J. Kelly for supplying us with numerical tables of the data presented here.

FIGURES

FIG. 1. The real (left column) and imaginary (right column) components of the free half–off–shell t–matrices for the spin singlet $^1P_1$ (upper) and $^1S_0$ (lower) channels. The solid line represents the "exact" Paris result, the dashed line, the parametrization considered here, and the dotted line, the zero density Hamburg t–matrix results.

FIG. 2. As for figure 1, but for the $(S = 1, T = 1)$ $^3P_0$ (upper) and $^3P_1$ (lower) channels.

FIG. 3. As for figure 1, but for the $(S = 1, T = 0)$ $^3S_1$ (upper), $^3D_1$ (middle) and $^3S_1$–$^3D_1$ (lower) channels.

FIG. 4. As for figure 1, but for the real (upper) and imaginary (lower) components of the $^3D_2$ channel.

FIG. 5. Central (upper) and spin–orbit (lower) optical model potentials for ^{12}C(p,p) at 200 MeV. The solid (dashed) line represents the medium modified (free) result.

FIG. 6. As for figure 5, but for ^{16}O at 200 MeV.

FIG. 7. Differential cross section (upper) and analyzing power (lower) for ^{12}C(p,p) at 200 MeV. The solid (dashed) line represents the medium modified (free) result. The data is from reference [11].

FIG. 8. As for figure 5, but for ^{16}O at 200 MeV. The data is from reference [12].

REFERENCES

[1] L. Ray, G. W. Hoffmann and W. R. Coker, Physics Reports **212**, 223 (1991); and references contained therein.

[2] A. Picklesimer, P. C. Tandy, R. M. Thaler and D. H. Wolfe, Phys. Rev. C **30**, 1861 (1984).

[3] H. F. Arellano, F. A. Brieva and W. G. Love, Phys. Rev. C **41**, 2188 (1990); Phys. Rev. C **42** 1782 (1990); Phys. Rev. C **43**, 2734 (1991); H. F. Arellano and W. G. Love, Phys. Rev. C **45**,759 (1992).

[4] Ch. Elster and P. C. Tandy, Phys. Rev. C **40**, 881 (1989); Ch. Elster, T. Cheon, E. F. Redish and P. C. Tandy, Phys. Rev. C **41**, 814 (1990).

[5] F. A. Brieva and J. R. Rook, Nucl. Phys. A **291**, 299, 317 (1977); W. Haider, A. M. Kobos and J. R. Rook, Nucl. Phys. A **480**, 1 (1988).

[6] W. G. Love and M. A. Franey, Phys. Rev. C **24**, 1073 (1981).

[7] H. V. von Geramb and K. Nakano, in "The Interaction Between Medium Energy Nucleons and Nuclei", AIP Conf. Proc. 97, edited by H. O. Meyer (AIP, New York, 1982), p. 44; L. Rikus, K. Nakano and H. V. von Geramb, Nucl. Phys. A **414**, 413 (1984).

[8] K. Nakayama, S. Krewald, J. Speth and W. G. Love, Nucl. Phys. A **431**, 419 (1984); K. Nakayama and W. G. Love, Phys. Rev. C **38**, 51 (1988).

[9] L. Ray and G. W. Hoffmann, Phys. Rev. C **31**, 538 (1985); L Ray, Phys. Rev. C **39**, 2816 (1990).

[10] N. Yamaguchi, S. Nagata and J. Michiyama, Prog. Theo. Phys. **76**, 1289 (1986).

[11] H. O. Meyer *et al*, Phys. Rev. C **27**, 459 (1983); and references contained therein; P. Schwandt, private communication.

[12] H. Seifert *et al*, Phys. Rev. C **47**, 1615 (1993); and references contained therein; J. J. Kelly, private communication.

[13] G. Bertsch, J. Borysowicz, H. McManus and W. G. Love, Nucl. Phys. A **284**, 399 (1977).

[14] A. M. Kobos, B. A. Brown, R. Lindsay and G. R. Satchler, Nucl. Phys. A **425**, 205 (1984).

[15] Dao T. Khoa and W. von Oertzen, Phys. Letts. B **304**, 8 (1993).

[16] J. P. Jeukene, A. Lejeune and C. Mahaux, Phys. Rev. C **16**, 80 (1977).

[17] H. V. von Geramb, K. Amos, L. Berge, S. Bräutigam, H. Kohlhoff and A. Ingermarsson, Phys. Rev. C **44**, 73 (1991).

[18] M. Lacombe, B. Loiseau, J. M. Richard, R. Vinh Mau, J. Côté, P. Pirès, and R. de Tourreil, Phys. Rev. C **21**, 861 (1980).

[19] J. Raynal, computer code DWBA91 (unpublished).

[20] M. I. Haftel and F. Tabakin, Nucl. Phys. A **158**, 1 (1970).

[21] P. J. Dortmans and K. Amos, J. Phys. G **17**, 901 (1991).

[22] P. J. Dortmans, Ph. D. thesis, University of Melbourne, 1992 (unpublished).

[23] J. W. Negele, Phys. Rev. C **1**, 1260 (1970).

Fig 1

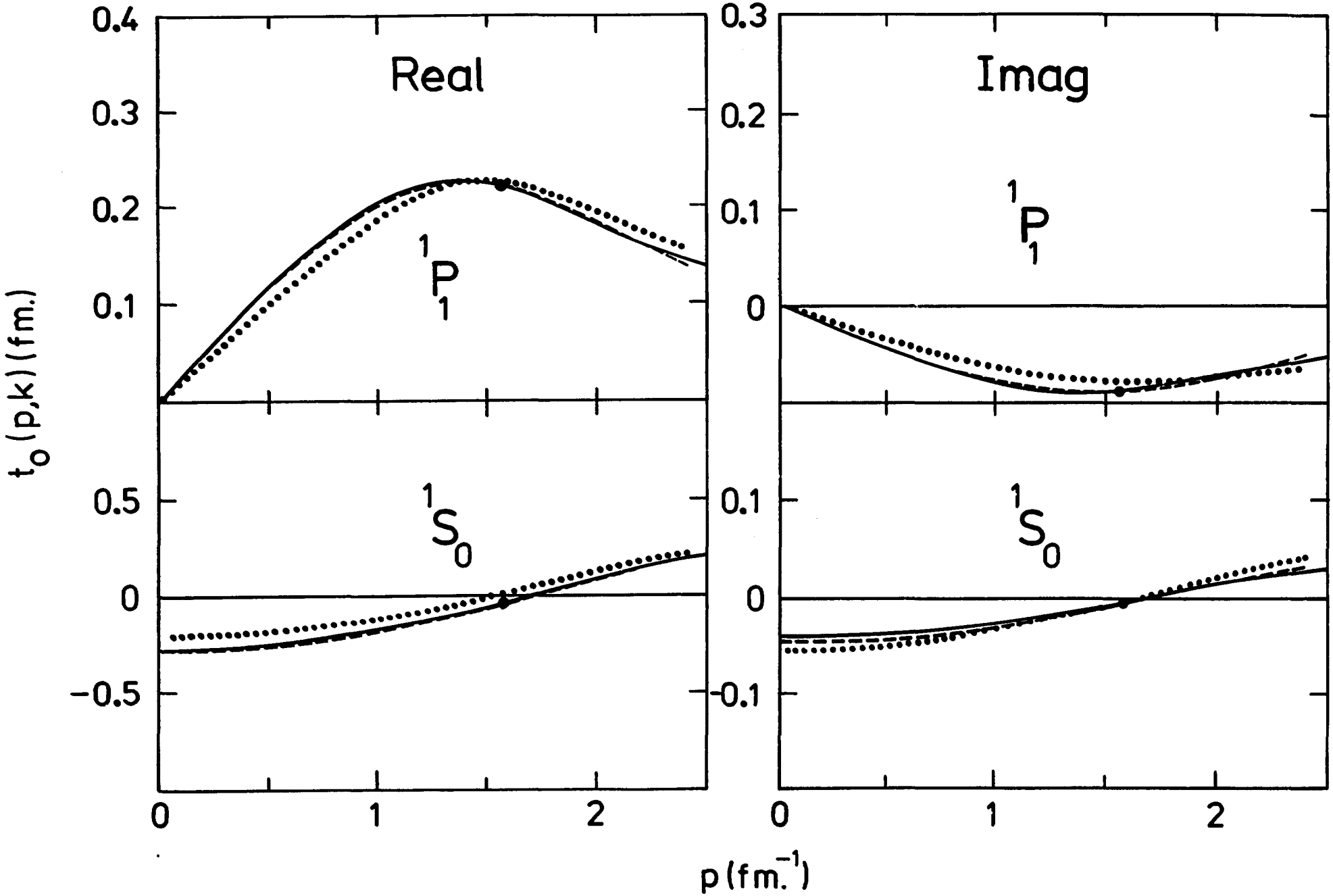

Fig. 2

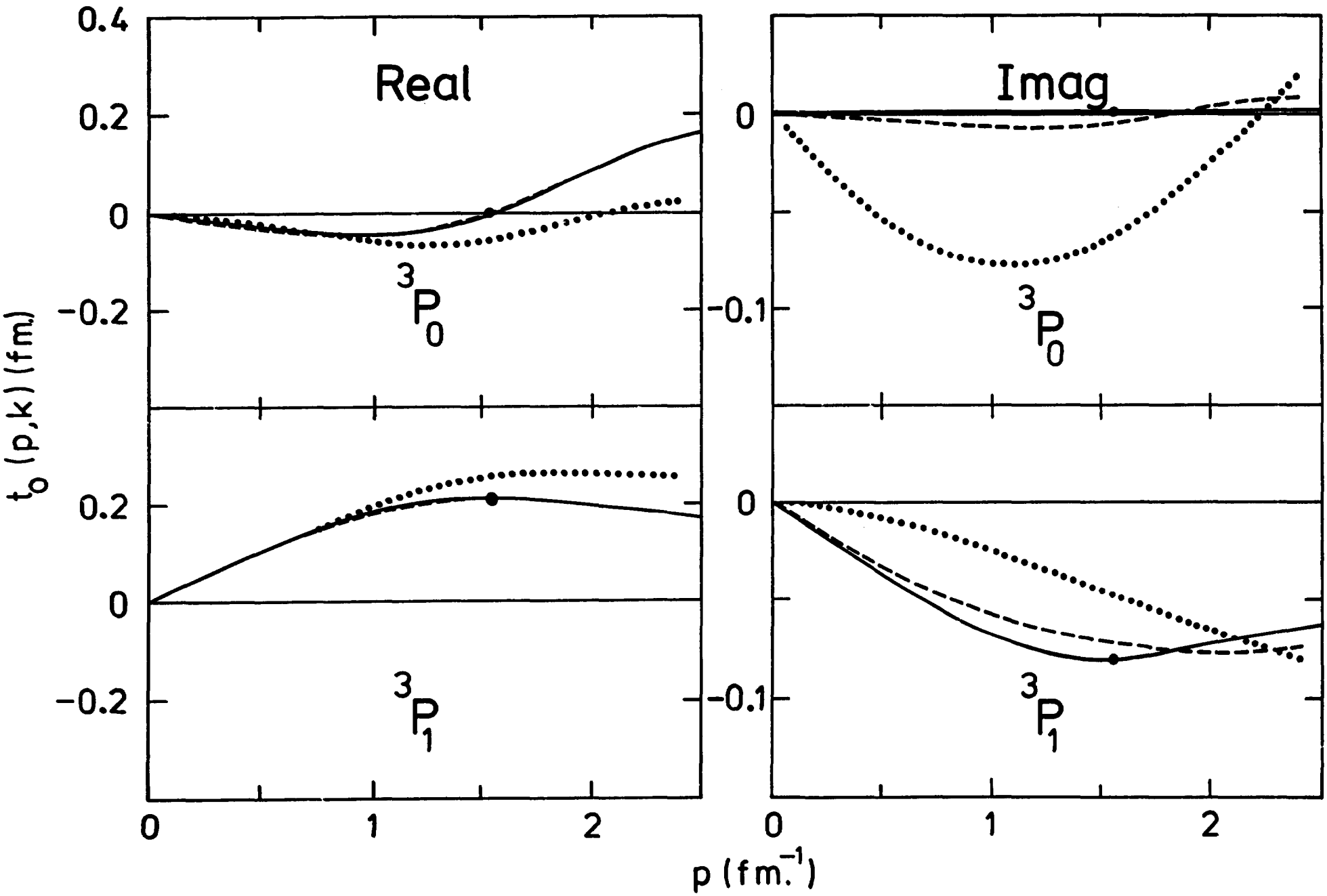

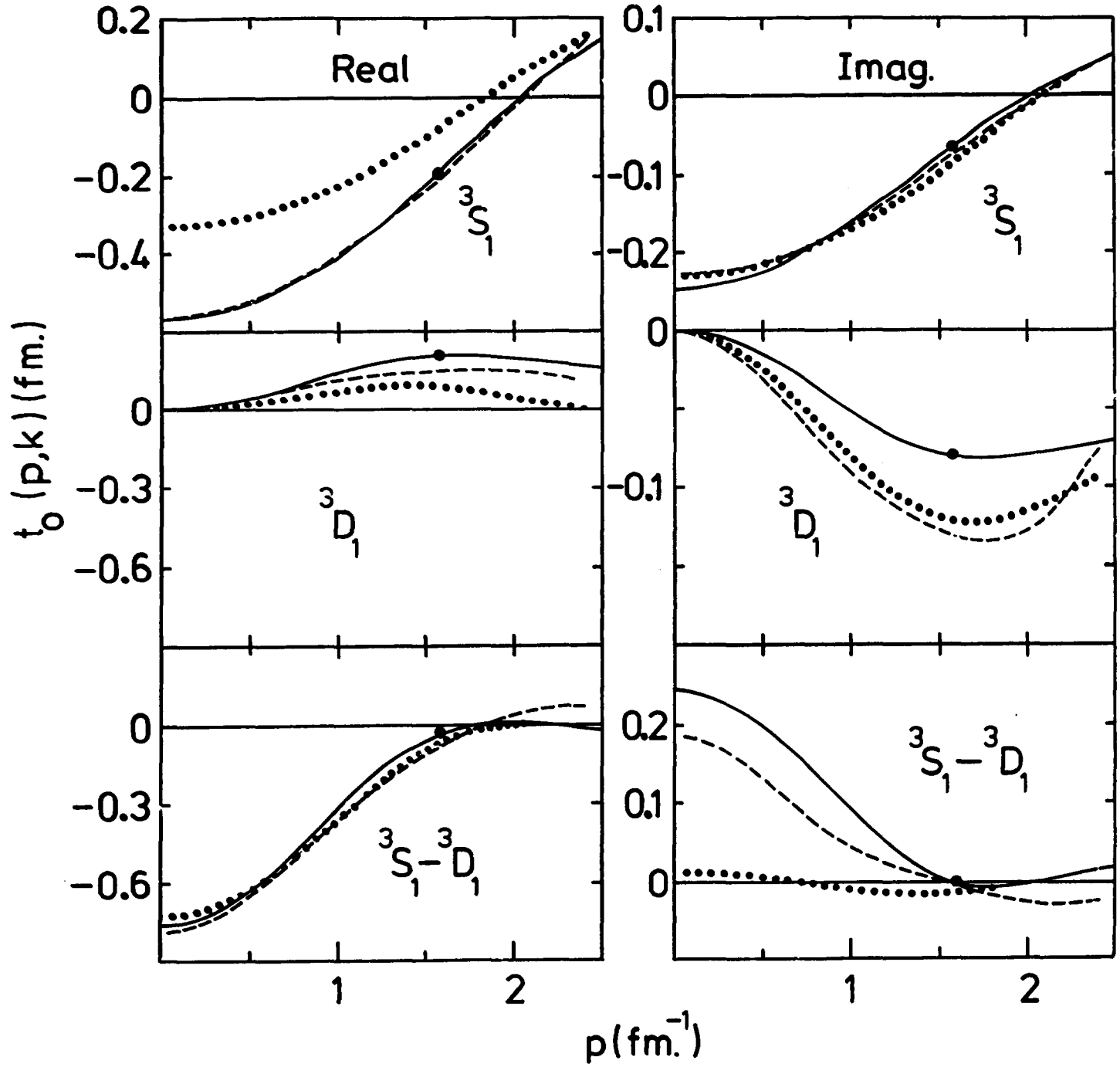

Fig. 3

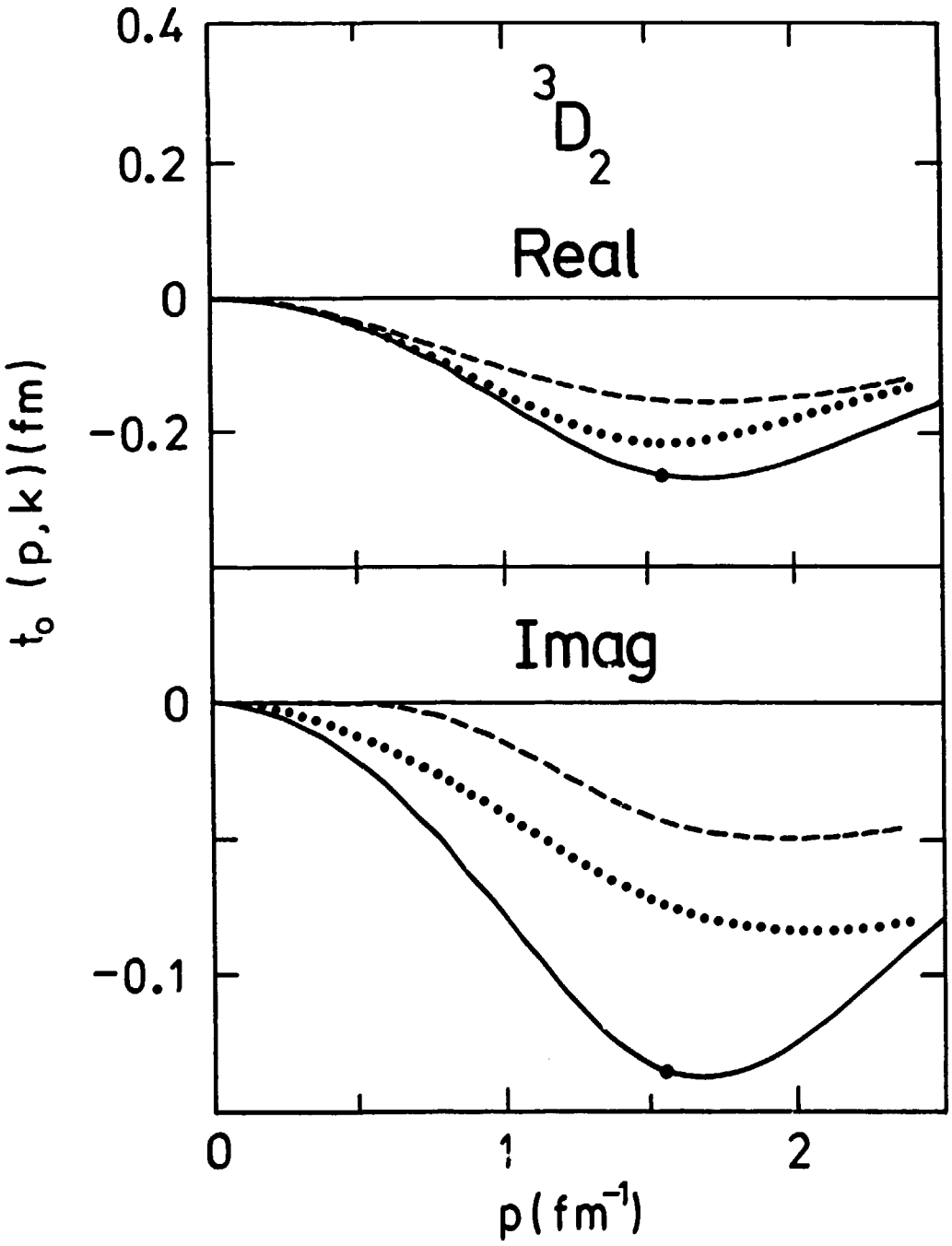

Fig. 4

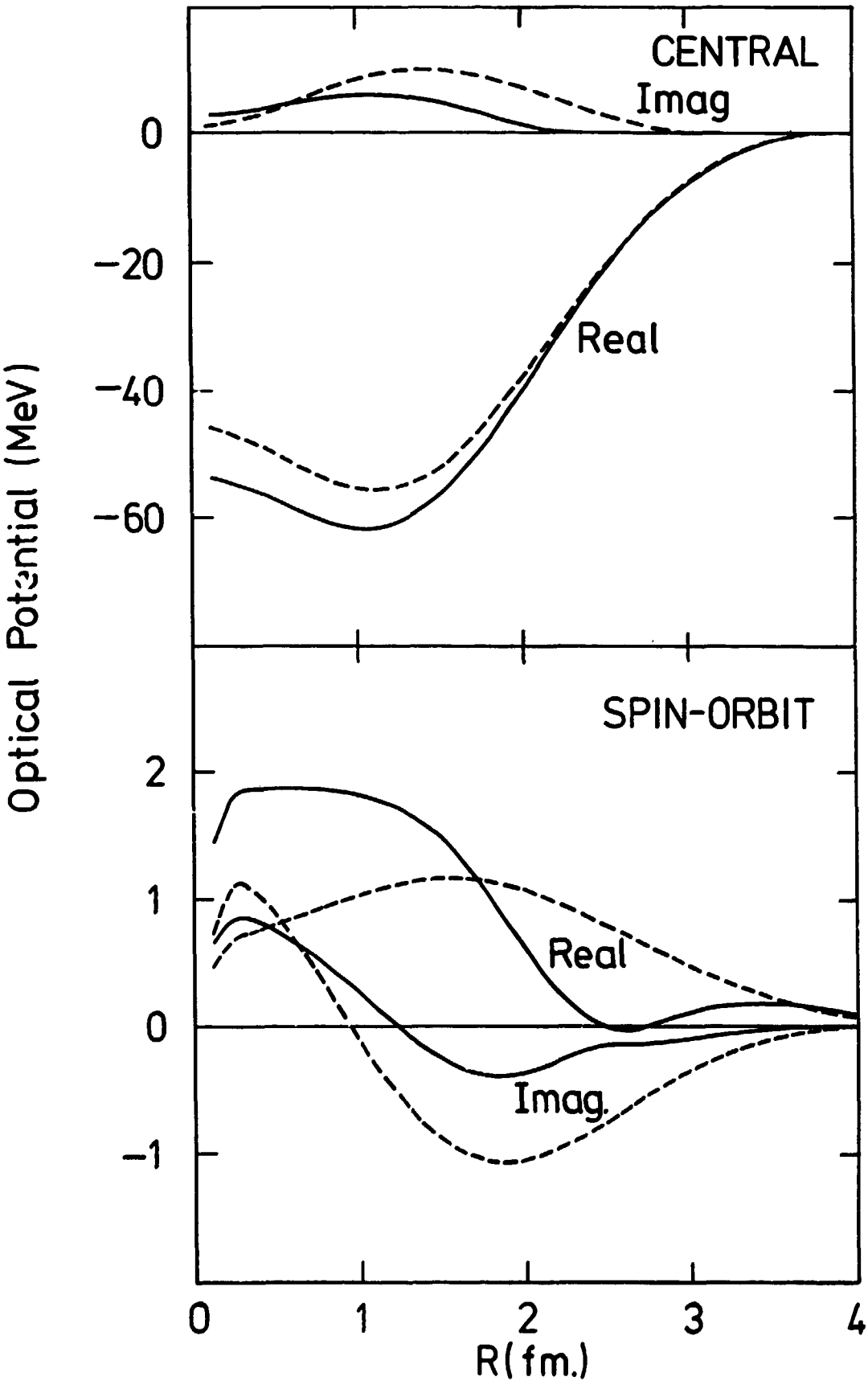
CENTRAL
Imag
Real
0
−20
−40
−60
SPIN-ORBIT
Real
Imag.
2
1
0
−1
0
1
2
3
4
R(fm.)
Optical Potential (MeV)

Fig. 5

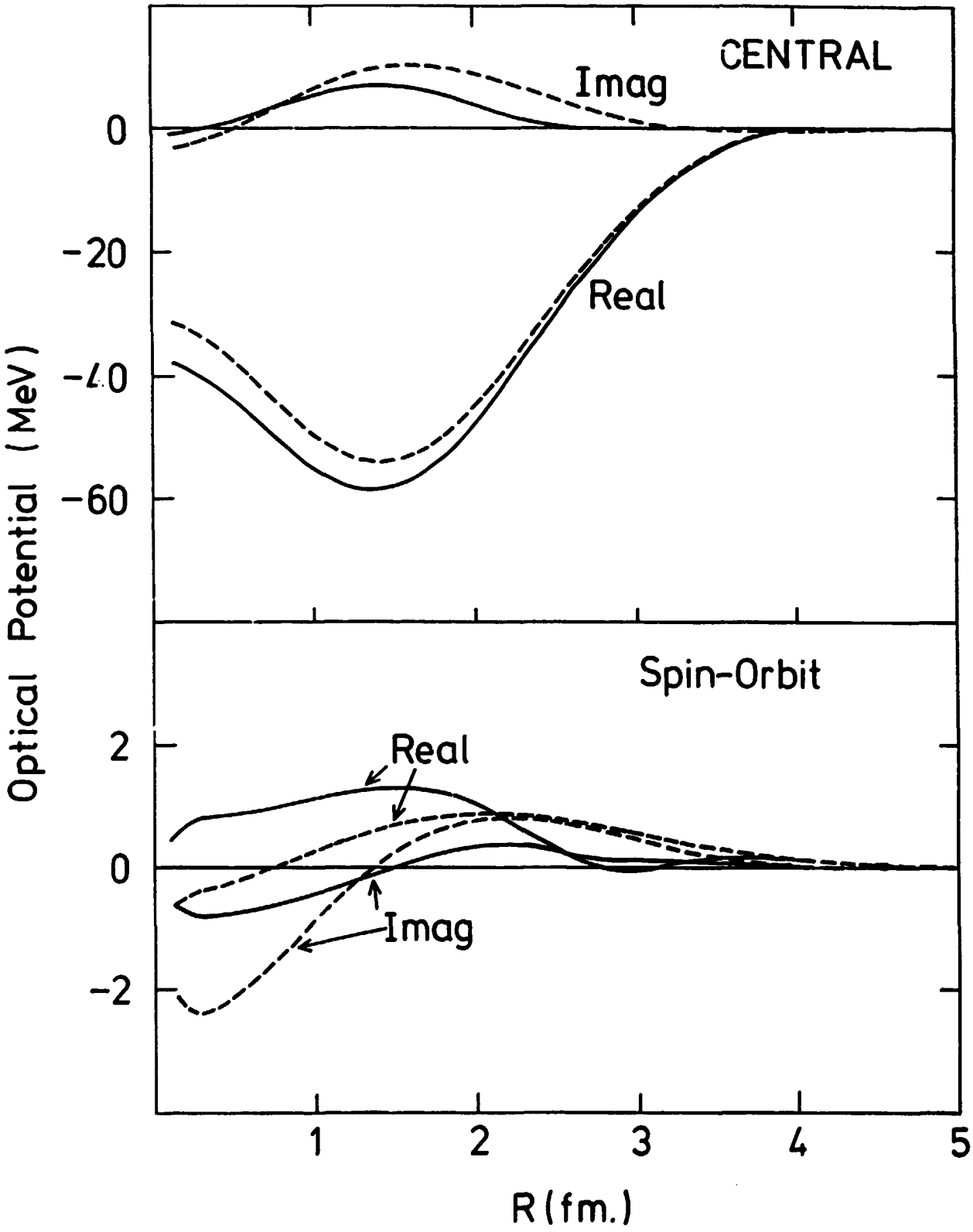
CENTRAL
Imag
Real
0
-20
-40
-60
Optical Potential (MeV)
Spin-Orbit
Real
Imag
2
0
-2
1
2
3
4
5
R (fm.)

Fig. 6

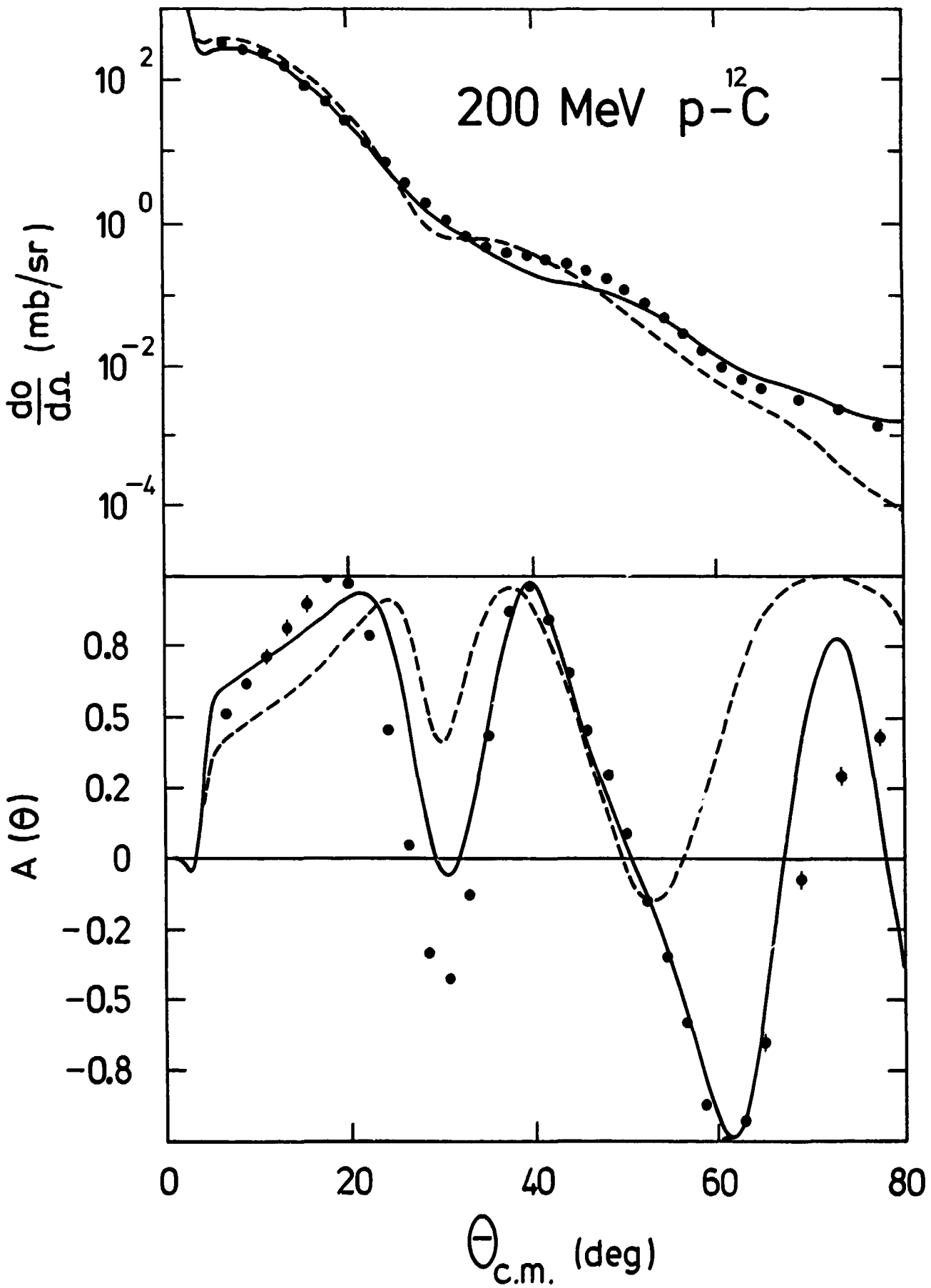
200 MeV p-12C
dσ/dΩ (mb/sr)
10 2
10 0
10 -2
10 -4
A (θ)
0.8
0.5
0.2
0
-0.2
-0.5
-0.8
0
20
40
60
80
θc.m. (deg)

Fig. 7

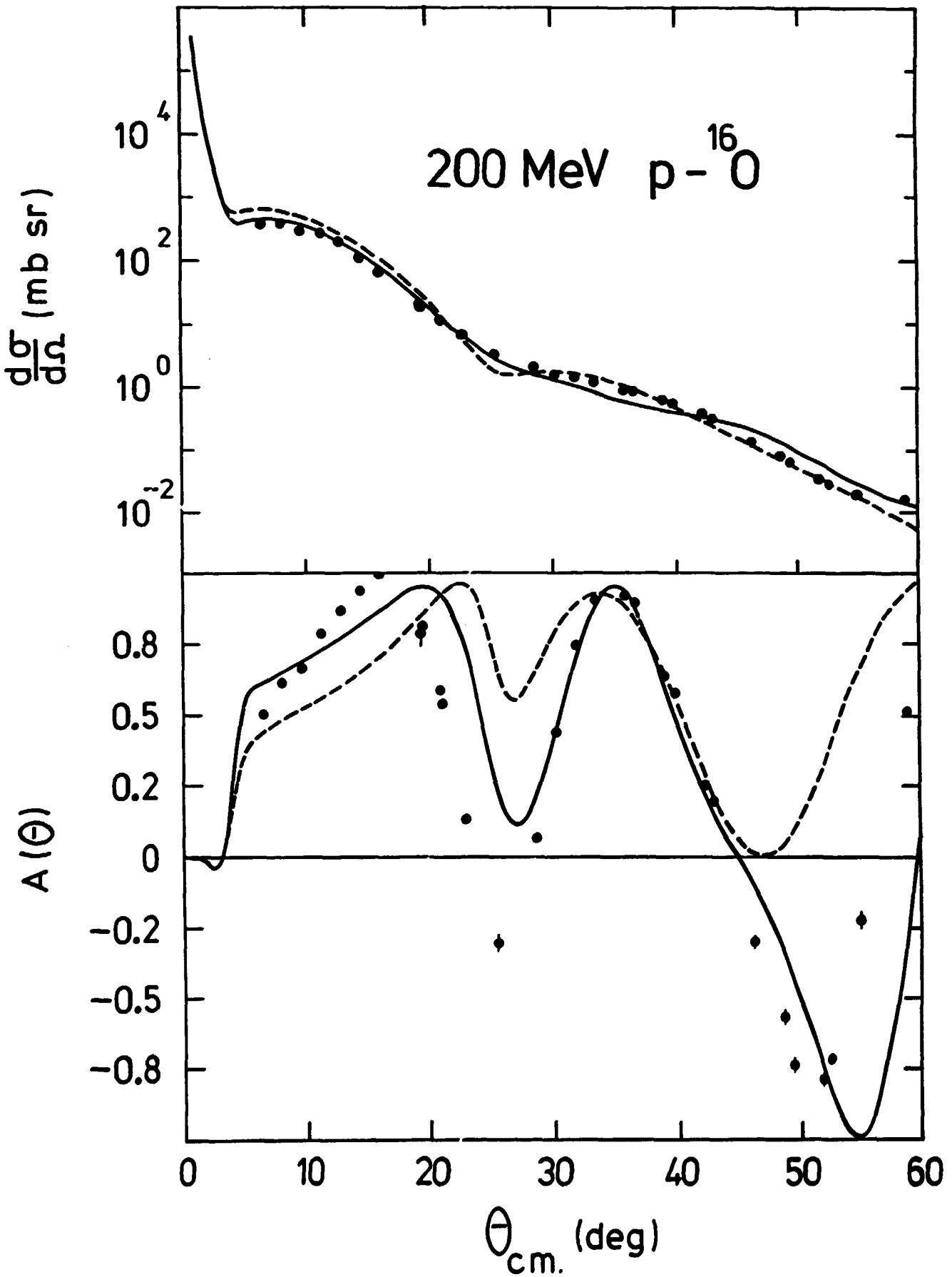
200 MeV p - 16O
dσ/dΩ (mb sr)
10^4
10^2
10^0
10^-2
A(Θ)
0.8
0.5
0.2
0
-0.2
-0.5
-0.8
0
10
20
30
40
50
60
Θcm. (deg)

Fig. 8